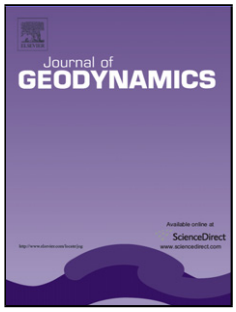

Title: Monitoring geodynamic activity in the Victoria Land, East Antarctica: evidence from GNSS measurements

Authors: A. Zanutta, M. Negusini, L. Vittuari, P. Cianfarra, F. Salvini, F. Mancini, P. Sterzai, M. Dubbini, A. Galeandro, A. Capra

PII: S0264-3707(17)30019-4
DOI: http://dx.doi.org/doi:10.1016/j.jog.2017.07.008
Reference: GEOD 1501

To appear in: *Journal of Geodynamics*

Received date: 14-2-2017
Revised date: 20-7-2017
Accepted date: 25-7-2017

Please cite this article as: Zanutta, A., Negusini, M., Vittuari, L., Cianfarra, P., Salvini, F., Mancini, F., Sterzai, P., Dubbini, M., Galeandro, A., Capra, A., Monitoring geodynamic activity in the Victoria Land, East Antarctica: evidence from GNSS measurements.Journal of Geodynamics http://dx.doi.org/10.1016/j.jog.2017.07.008

Monitoring geodynamic activity in the Victoria Land, East Antarctica: evidence from GNSS measurements

A. Zanutta [a,*], M. Negusini [b], L. Vittuari [a], P. Cianfarra [c], F. Salvini [c], F. Mancini [d], P. Sterzai [e], M. Dubbini [f], A. Galeandro [d], A. Capra [d]

[a] Dipartimento di Ingegneria Civile, Chimica, Ambientale e dei Materiali - Università di Bologna;

[b] Istituto di Radioastronomia – Istituto Nazionale di Astrofisica, Bologna;

[c] Dipartimento di Scienze Geologiche, Università degli Studi Roma Tre;

[d] Dipartimento di Ingegneria Enzo Ferrari - Università degli Studi di Modena e Reggio Emilia, Modena;

[e] Dipartimento di Geofisica della Litosfera - Istituto Nazionale di Oceanografia e Geofisica Sperimentale, Trieste.

[f] Dipartimento di Storia Culture Civiltà – Università di Bologna;

*Corresponding author at: Dipartimento di Ingegneria Civile, Chimica, Ambientale e dei Materiali - Università di Bologna, V.le Risorgimento 2 – 40136 Bologna, Italy.

E-mail address: antonio.zanutta@unibo.it (A. Zanutta).

Highlights

- Geodynamic activity in the Victoria Land is evidenced from VLNDEF network measurements;
- By a preliminary comparison, the ICE-6G_C-VM5 and W12A_v1 GIA models overestimate uplift rates with respect to GPS-derived ones;
- The up component confirms the presence of active extensional/transtensional faulting along the SE segment of the Tucker Fault and the central segment of the Leap Year Fault.

Abstract

GNSS networks in Antarctica are a fundamental tool to define actual crustal displacements due to geological and geophysical processes and to constrain the glacial isostatic models (GIA). A large network devoted to the detection and monitoring of crustal deformations in the Northern Victoria Land (Victoria Land Network for DEFormation control -

VLNDEF), was monumented during the 1999-2000 and 2000-2001 field campaigns, as part of Italian National Program for Antarctic Research and surveyed periodically during the Southern summer seasons.

In this paper, GPS observations of VLNDEF collected over a more than 15-year span, together with various selected POLENET sites and more than 70 IGS stations, were processed with Bernese Software, using a classical double difference approach. A solution was obtained combining NEQs by means of ADDNEQ2/FODITS tools embedded in Bernese Software. All the Antarctic sites were kept free and a subset of 50 IGS stations were used to frame VLNDEF into ITRF2008. New evidence provided by analysis of GPS time series for the VLNDEF network is presented; also displacements along the vertical component are compared with the recently published GIA models. The absolute velocities indicate an overall displacement of the northern Victoria Land region along the south-east direction (Ve=10.6 mm/yr, Vn=−11.5 mm/yr) and an average uplift rate of Vu=0.5 mm/yr. Two GIA models have been analyzed: ICE-6G_C-VM5a proposed by Argus et al. (2014), Peltier et al. (2015) and W12A_v1 by Whitehouse et al. (2012a,b). Up rates, predicted over the VLNDEF sites by the mentioned GIA models, have been extracted and compared with those observed. A preliminary comparison with GPS-derived vertical rates, shows that the Victoria Land ICE-6G_C-VM5 and W12A_v1 GIA models predict overestimated uplift rates of 0.7 and 0.9 mm/yr weighted mean residuals respectively. The mean horizontal relative motions within the Victoria Land (VL) area are in most cases negligible, while only a few points exhibit horizontal velocities greater than the confidence level. Such a residual horizontal velocity field could represents some of the tectonic characteristics affecting VL, characterized by block faulting, tilting along NE striking and SE dipping extensional faults. Uplift rates, highlighted in the present paper depict a well defined spatial pattern in the investigated areas. Northward, all sites show a general positive trend up to 2.3 mm/yr. In the central and southern areas small negative trends (up to -1.3 mm/yr) were detected in the vertical displacements. Only the site VL06, located atop the Mt. Melbourne volcano, does not concord with such a general reading, as it is representative of the volcanic complex's evolution. Observed and predicted uplift rates increase westward (inland) where the ice-load increases. The same behavior is predicted southward by the GIA models; whereas, GPS values decrease toward the south pole, due to the movements of a few sites reflecting the neotectonic phenomena acting in the Victoria Land region.

Key words

GNSS, Victoria Land, Antarctica, crustal deformation, glacial-isostatic adjustment, Neo-tectonics

1 - Introduction

The GNSS technique is widely employed to detect crustal deformations and to characterize the kinematics of the Earth's lithosphere (on small medium and large scale) all over the world.

Antarctica is a hostile continent almost entirely covered by ice where GNSS data are sparse, as well as incredibly difficult and expensive to collect due to the extreme conditions and difficulties with travel logistics. Only 0.18 % of the Antarctica is ice-free and suitable for GNSS installation on stable outcrops (Burton-Johnson et al., 2016). This produces an uneven distribution of the GNSS stations, which are mainly located along coastal areas.

The northern Victoria Land area (NVL; Fig. 1) is located in the East Antarctic craton. While the East Antarctic is considered a stable continent surrounded by passive margins, NVL is characterized by evidence of neotectonic movements: block faulting, as well as, tilting along NE striking and SE dipping extensional faults connected to the fracture system of the Balleny and Tasman Fracture zones (e.g.,Salvini et al., 1997, 1999). GNSS measurements may be an efficient tool for highlight the geodynamics and neotectonics of NVL through the detection of crustal deformation. The analysis of GNSS data derived from continuous or discontinuous networks provides three-dimensional information about the position and movements of the stations. However, the observed solid Earth deformation includes several signals produced by different geophysic phenomena which are often difficult to separate. Recent works show that the main displacements detected in the NVL are consistent with those of the East Antarctic plate (Capra et al., 2008). A standard approach to highlighting tectonic movements is based on the residual rate evaluation obtained by the Euler pole estimation and the subtraction of the plate movement from the absolute site rates. The residual velocities should reflect deformation, due to glacial isostatic adjustment (GIA) horizontal components which, in Antarctica, are not negligible (King et al., 2016). Furthermore, residual rates may be biased by the number, quality of data delivered and geographical distribution of the GNSS stations used to compute the Euler Pole.

The task of detecting such a residual velocity field, on a selected spatial scale, was made easier by the analysis of continuous GNSS time series, which were provided, from permanent stations in Antarctica, on decadal timescales. The drawback of using permanent GNSS stations to detect surface motions is the limited number and density of stations whenever a detailed picture of regional deformation phenomena is sought.

In addition discontinuous GNSS campaigns with a long series of data, like those with high spatial station densities carried on VLNDEF network, are able to produce reliable results for the characterization of the present-day geodynamics; they also may be able to shed light on the residual velocities which are due to active tectonic structures in

the region. Eventually GNSS networks can be used to constrain and test the reliability of GIA models (King et al., 2010, 2014; Steffen and Wu, 2011).

Previous studies have attributed the main horizontal displacement field within Antarctica to a rigid plate rotation and deformation related to the change in ice-loading (Amalvict et al., 2009; Argus et al., 2014; Bevis et al., 2009; Bouin and Vigny, 2000; Torsvik et al., 2008; Thomas et al., 2011). The ice melting began at the end of the last ice age and produced a slow crustal deformation which is affected nowadays by the alteration of glacier flows, themselves due to climate change and neo-tectonic movements. Even the breakup of ice shelves produces regional variations in the displacement pattern: this happened in the Northern Antarctic Peninsula following the 2002 breakup of the Larsen ice shelf, which was due to the combined effects of solid Earth's elastic response ~~of~~ and the viscoelastic process roughed on by the recent ice unloading (Nield et al., 2014; Thomas et al., 2011).

Deformations associated with earthquakes contribute to the general displacement field, although large-magnitude seismic activity is quite limited in Antarctica (Reading, 2007). Deformations associated with large-magnitude earthquakes, such as: the A98 which occurred in 1998, 500 km north of the Dumont d'Urville French station (Nettles et al., 1999), in 2004, the Macquarie Ridge earthquake (Watson et al., 2010); in 2004, the Sumatra earthquake; in 2010, the earthquake in Chile; and finally, in 2011, the Tōhoku earthquake in Japan, are capable of inducing modifications in superficial crustal movements in Antarctica. The nonlinear, post-seismic deformations which occurred in Antarctica could be misinterpreted as concerns secular geodetic estimates of plate motion and even the GIA rate. King and Santamarìa-Gòmez (2016) attributed to the 1998 Macquarie Ridge's earthquake the cessation of movement in a northern direction as well as a reduction in speed of movement towards the east and up in East Antarctica. This paper presents evidence of crustal deformations in VL, obtained from recent data collected under the auspices of the VLNDEF project. Site velocities now refer to a larger period; from DOY 349 of 1998 to DOY 040 of 2015. Compared to previous works (Capra et al., 2007, 2008; Dubbini et al., 2010; Zanutta et al., 2008), the network time extension has been improved with additional measurements and more repetitions.

From the data processing, coordinates and velocities of the sites were estimated. With the aim of obtaining relative velocities, Euler pole and angular velocity of the Antarctic plate were evaluated inverting the GPS-derived motions of all VLNDEF sites together with IGS permanent stations located in Antarctica. A detailed analysis of the horizontal velocity components was made, and a possible interpretation provided, as regard the neotectonic characteristics of the VL region.

Vertical velocity components have been compared with those obtained by two GIA models: the ICE-6G_C-VM5a (Argus et al., 2014; Peltier et al., 2015; Professor W.R. Peltier's personal website http://atmosp.physics.utoronto.ca/~peltier/data.php), and the W12A_v1 model (Whitehouse et al., 2012b; http://cryolist.464407.n3.nabble.com/W12a-Glacial-Isostatic-Adjustment-model-for-Antarctica-td4025202.html).

2 - Data acquisition

The VLNDEF network, whose surveying is based on periodic campaigns, was established in 1999 (Capra et al., 2001, Mancini, 2001) and completely surveyed 5 times, even if some sub-network measurements have been performed more frequently over certain areas of interest for purposes mostly related to the investigation of local geodynamic phenomena. The GNSS sites are distributed over all VL, fixed in bedrock on iron pillars, where the antenna is mounted directly onto the marker.

Due to the hostile environment and ~~the~~ considerable distances (up to about 450 km) from the Mario Zucchelli Stations - MZS (where TNB1 GNSS station is located, Fig. 2), the collecting of GNSS measurements in VL poses several logistic difficulties, mostly because the majority of sites are only accessible by helicopters.

Since the beginning of the VLNDEF project, the simultaneous data acquisition sessions lasted at least 24hrs, typically 72-h, recorded by geodetic GNSS receivers powered by a set of batteries and solar panels. In order to minimize the effect of bias over time series, only a single model of choke ring antenna was used during the surveys of the sites. Up to the present day, 27 sites were surveyed in the VL and related time series produced on a regular basis.

In the 2014-15 Italian Antarctic expedition, the VL01, VL12, VL30 sites were transformed into permanent stations framed within the POLENET project (Polar Earth Observing NETwork, http://polenet.org/ accessed on December 2016). The locations of the GNSS sites are shown in Figure 1. The data base used in this study is summarized in Table 1.

Fig.1. GNSS Antarctic stations (IGS, POLENET) used in this paper. The VLNDEF network is represented in the upper - right inset.

Table 1 - GNSS sites in the VL region. For each year the number of daily observations is given. The last two columns indicate the accumulated total amount of daily observations (Tot) and the number of repetitions (Rep).

3 - GNSS data processing

The VLNDEF data, covering more than 15 years, were analyzed in a double-difference approach, using a modified version of the Bernese V.5.0 software (Dach et al., 2015), which enables the use of hydrostatic and wet Vienna Mapping Functions (VMF1; Boehm et., al 2006), as well as the Global Pressure and Temperature 2 (GPT2) model (Lagler et al., 2013). The implementation of such models allowed a better estimation of the Zenith Total Delay (ZTD), thus providing more reliable results in coordinate computation, particularly in the Antarctic regions. Given the availability of a long time series of observations, the whole dataset was completely reprocessed to obtain consistent and unbiased estimates of the geodetic parameters (Steigenberger et al, 2006, 2009; Tesmer et al., 2009; Rothacher et al., 2011).

A two-step analysis was implemented. Firstly, a "regional" solution was set-up: this step includes the data processing from the VLNDEF project, in addition to that provided by POLENET FTP0/4, FLM1/2/5 and ROB0/1/4 stations within the Antarctic framework, established by the use of a limited number of IGS permanent stations (CAS1, DAV1, DUM1, MAW1, MCM4. OHIG/OHI2, PALM, SYOG, VESL; Figure 1).

The subset of IGS stations was used to define the geodetic datum, performing a minimum constraint solution, applying a No-Net Translation (NNT) condition during the NEQ stacking process. During this step, daily solutions were obtained.

Secondly, a "global" solution was set-up using data from the permanent Antarctic stations, coupled with the global network of more than 70 IGS stations, selected following criteria of homogeneity, geographical distribution and length of the observation. Products derived from the IGS repro1 campaign (ftp://cddis.gsfc.nasa.gov/gps/products/repro1), including IGS station coordinates, satellite orbits and Earth Orientation Parameters, were used, together with absolute phase-center corrections, applied for both satellite and receiver antennas. Corrections for solid-earth ocean and pole tides were applied following the IERS2013 Conventions; FES2004 (Letellier, 2004) + TPXO.6.2 (Egbert and Erofeeva, 2002), including the CoM, correction for the Earth's motion due to ocean tides was applied.

The geodetic datum was defined by a NNT condition, performing a minimum constraint solution and fixing a sub-set of approximately 50 IGS stations, which were chosen as having the most reliable and stable a priori coordinates into ITRF2008 (Altamimi et al., 2011). Even during this step, daily solutions were computed. Further details about the implementation of the "global" solution can be found in Negusini et al. (2016).

Finally, the NEQs obtained by the "global" process were combined with those taken from the "regional" weekly solutions. The weekly NEQs were combined with Bernese 5.2 (Dach et al. 2015), using the time series analysis routine FODITS (Find Outliers and Discontinuities in Time Series), embedded in the Bernese GNSS Software (Dach et al., 2015; Ostini et

al., 2008, 2010; Ostini, 2012). FODITS is able to identify discontinuities in station velocities and ~~to~~ estimate representative periodic functions. All three components of coordinate time series are processed together in a fully combined mode. The program FODITS verifies the significance of lists of predefined events: such as a list of equipment changes, as well as a list of worldwide registered earthquakes (derived from the database of the U. S. Geological Survey Earthquake Hazards Program); at the same time, FODITS identifies discontinuities and outliers in the time series. It identifies the stations affected by worldwide earthquakes following the model proposed by Delle Donne et al. (2010). Within FODITS, station velocities are assumed to be linear in time while the time series are analyzed station by station. In order to simplify the analysis and reduce the processing time, coordinate time series of different stations are assumed to be independent.

Seasonal signals (annual and semi–annual periods) are estimated and their related components checked for significance (Dong et al., 2002). No time correlation is assumed between the data points of the time series. Only the space correlations (between the North, East, and Up component) are taken into account. The full covariance matrix is considered in a consecutive network solution using ADDNEQ2 after the time series analysis by FODITS. By means of this procedure embedded in the Bernese software 5.2 no VLNDEF stations showed significant discontinuities, nor change in rate. In the last ADDNEQ2 run, all the Antarctic sites were kept free and the same subset of 50 IGS stations were used to frame VLNDEF into ITRF2008.

It is well known that Bernese formal errors (RMS) are underestimated when analyzing big amounts of data (Dietrich et al., 2005; Márquez-Azúa et al., 2004; Mao et al., 1999; Saleh, Becker, 2015; Williams, 2003; Williams et al., 2004; Zhang et al., 1997). For long time series of data, different tools are available for studying both spatial and temporal correlations, but these methods are not useful for campaign data. Argus et al (2014) estimated the uncertainty in the GPS site velocities from the effective time period of observations. They take the standard error in the vertical component to be 10 mm, divided by the effective time period of observations in yrs and to be 4.5 mm divided by the effective time period of observations in the horizontal components. Errors in episodic campaigns are assumed to be 33 per cent larger than in continuous observations. Using this method, we are able to assign more reliable uncertainties to the velocity components of the VLNDEF sites, as shown in Table 2 and in Figure 2.

Fig. 2. Victoria Land absolute velocities.

The solution appears to be consistent with a general motion toward south-east. The vertical (color-coded) mean velocities depict a weak uplift of 0.5 mm/yr. VL06 shows a positive trend compatible with the evolution of the Mt. Melbourne volcanic complex on which it is installed. In the Ross Sea coastal region, few VLNDEF sites seem to be affected by block faulting, tilting along NE striking and SE dipping extensional faults, all related to the Ross Sea embayment (Figure 7).

Table 2 – List of VLNDEF sites with coordinates, absolute and relative velocities along the north and east components (from DOY 349 of 1998 to DOY 040 of 2015) and their estimated uncertainties ($\pm\sigma$).

The Euler pole and the angular velocity of the Antarctic plate were calculated by inverting the GPS-derived motions of all VLNDEF sites together with IGS and POLENET permanent stations located in Antarctica (CAS1, DAV1, DUM1, FLM5, FTP4, MAW1, MCM4, OHI2, PALM, ROB4, SYOG, VESL) than compared with the location provided within the definition of the ITRF2008 (Altamimi et al., 2012; see Tab. 3). Afterward, relative movements among stations were determined by subtracting the rigid body movement of the continent, derived by applying the above mentioned Euler Pole, from the absolute VLNDEF site velocities (Fig. 3).

This computation, including the VL sites, well constrains the motion of the Antarctica plate and tends to minimize the relative velocities among the VLNDEF stations. In this way the computed residuals are expected to be smaller than the previously used (Dubbini et al, 2010). As a result, this paper shows reduced residual velocities that cannot be ascribed merely to improvements in accuracy, nor to dramatic reductions (approx. 50%) in tectonic activity in the last few years. Even within this restriction, the residual velocities largely confirm the tectonic framework which is active in VL, as proposed by Dubbini et al. (2010) and Zanutta et al. (2008).

Table 3 - Geographic Coordinates and the rotation rate of the Euler pole position projected onto the Southern Hemisphere. ITRF2008 from Altamimi et al. (2012); VLNDEF, this work.

Fig. 3. Victoria Land horizontal relative velocities with respect to VLNDEF plate model. The very small displacement vectors indicate the general agreement of the VLNDEF model with the Antarctic plate movement, except for some points of the northern part, which confirm the influence of displacements due to tectonic patterns across the region.

4 – Results: a comparison between GIA models and observed data

In this work, the vertical change predicted by GIA models are compared to the GPS observations, considered as an independent means, to verify the GIA local accuracy.

ICE-6G_C (VM5a viscosity model) is a global postglacial rebound model constrained to fit geological and geodetic observations (Argus et al., 2014; Peltier et al., 2015). This is a laterally homogeneous model with a simplification of viscosity structure VM5 (upper mantle viscosity 0.5×10^{21} Pa s; lower-mantle viscosity $\eta_{LM} = 10 \times 10^{21}$ Pa s.) and a lithospheric thickness h = 100 km. A detailed comparison with observed GNSS site velocities in Argus et al. (2014), demonstrates that in Antarctica the model well fits the GNSS uplift rates, with a weighted mean residual of -0.31 mm/yr. The GIA model predicts a little larger uplift than observed. Purcell et al. (2016) showed that the radial uplift rates of Peltier et al. (2015) were too high along Antarctic coastline and on the eastern side of the Ross Ice Shelf with an estimated bias of 5 mm/yr. The same authors, by means of CALSEA software package, produced the ICE6G_ANU which minimize these disagreements.

W12A_v1 (Whitehouse et al., 2012a,b) is an Antarctic GIA model that covers spatially from 90S to 55S, with 0.5 degree grid intervals in both longitude and latitude. The deglacial ice model used to guide the W12a model includes an Antarctic component (Whitehouse et al. 2012a) and a far field component embedded in the ICE-5G model (Peltier, 2004). The W12A_v1 model 'B' (best) has been adopted, corresponding to lithospheric thickness h = 120 km, upper-mantle viscosity $\eta_{UM} = 1 \times 10^{21}$ Pa s, and lower-mantle viscosity $\eta_{LM} = 10 \times 10^{21}$ Pa s.

The comparison of up rates from GIA models and GNSS observations requires further consideration. The GIA models refer to displacements under several assumptions related to the lithosphere state: ice-loading/unloading history; mantle viscosity; global / regional isostatic and/or Earth models (Peltier, 2004; Simon et al., 2010). Furthermore, ice models use gravity data, geoid anomalies and relative sea level (RSL) fluctuations during the last 20 kyr. RSL variation is strongly dependent on ice sheet advances and retreats, and is poorly sensitive to mantle viscosity (Mitrovica and Vermeersen, 2002). The GIA model output includes the influence of sea-level changes and induced perturbations to Earth rotation (Mitrovica and Milne, 2003; Mitrovica et al., 2005). Both GIA models considered in this work use, as a frame of reference, the Earth's centre (CE); whereas, GPS solutions define Earth's frame of reference, using the velocity of mass centre (CM) in ITRF2008. The use of the ITRF2008 in Antarctica produces a bias in the vertical motion of up to 0.5 mm/yr (Argus, 2012). Argus et al., 2014, estimated a positive bias of 0.48 mm/yr at the southernmost latitudes, which

can affect the comparison between GNSS-derived vertical rates and up rates predicted by the ICE-6G_C-VM5a model. In particular, the GIA models overpredict uplift rates compared to those from GNSS ITRF2008. Whitehouse et al. (2012b) highlight the fact that the W12a_V1 GIA model does not include the effect of present-day surfaces mass-transport upon the centre of mass. The combined effect of such phenomena amounts to 0.5 mm/yr (Klemann, Martinec 2011; Rietbroek et al., 2012). Moreover, in the comparison between GPS vertical rates and GIA model response issues, the effects of elastic deformations and rapid changes in polar motion during the last two decades should also be taken into account. As suggested by Riva et al. (2016), the increase in melt rates, which occurred over the last two decades, produced significant variations of deformation rates not only in the areas nearest to those involved in the ice-melting process, but also in the far field as a global solid earth response. In particular, the recent acceleration is connected to an increase in loss of mass from the Greenland and the Antarctic ice sheets. Vertical displacement, due to the above mentioned phenomena, could introduce a bias as regards the GIA model, the latter being representative of deformations on a century scale. Riva et al. (2016), determined the solid earth elastic response by including recent assessments of ice-loss for glaciers as well as the Greenland and the Antarctic ice-sheets. The resulting time series of vertical land motion on a global scale showed the largest uplift values at the location of melting sources, while negative responses as well as smaller uplift rates (up to 1mm/yr during the last decade) were identified in the far field where several competing processes may interact. However, the Northern Victoria Land does not fall within the areas that are most affected by elastic responses to recent ice-melt processes (a few tenths of mm/yr were predicted using available models). In addition, the quantification of ice-loading changes is not an easy task. Thus, we decided to ignore the elastic responses, induced over the VLNDEF sites within the time-span of measurements, in order to avoid the correction of vertical rates by small values, themselves characterized by unknown level of accuracy. King and Watson (2014) introduced an additional, relevant point to the discussion of put forth by the present paper. They showed the potential effect introduced by the rapid motion of the rotation pole starting in around 2005. Worldwide, a bias of up to tenths of mm/yr could affect estimates of vertical velocity detected since 2005 with respect to the longer-term deformation picture. Especially for those areas where anomalies to the average pattern are expected due to the recent rapid polar motion, site velocities from geodetic observations collected since 2005 could not be representative of deformation rates at century scale. Geodetic measurements on VLNDEF sites commenced in 1998. Thus, time series are less affected from incorrect modelling of polar motion in recent years. King and Watson provided a modelled deformation pattern within the period 2001-2015. In the investigated area the magnitude of unmodelled terms is less than half mm over the whole period.

However, over long-term geodetic measurements, the presence of residual non-linear signals could affect the level of uncertainty of site velocities, due to a combination of bias and noise. A correction to the IERS pole tide model would be able to take into account such non-linear phenomena (King and Watson 2014).

To estimate the level of agreement between the observed uplift rates and those predicted by the GIA models, statistical parameters are evaluated and shown in Table 4. In particular, Table 4 reports the weighted mean (WM) and the weight root mean square (WRMS) values of differences as proposed by Martín-Español et al., 2016.

In the NVL region the observed vertical rates range between +2.9 mm/yr and -1.3 mm/yr (negative rate at VL04 site). The absolute vertical velocities reveal an average uplift across the VL with a mean value of 0.5 mm/yr (Fig. 4). The sites, VL12, VL29 and VL30 exhibit the highest values, respectively, 1.7, 2.9 and 2.3 mm/yr (Tab. 2, 4). Figure 4 provides a visual comparison between the predicted vertical rates of the three models and the uplift rates measured by GPS observations.

Fig. 4. Predictions by postglacial rebound models across the NVL and GPS observed uplift rates. a) ICE-6G_C-VM5a (Argus et al., 2014); b) W12A_v1 (Whitehouse et al., 2012a,b). The circles indicate the difference ranges between the predicted and the observed vertical rates.

The overall predicted rates by the mentioned models are very similar in NVL. At the present time, all of them are revealing maximum and minimum uplift rates in the southern and northern areas, respectively, with values which are a little larger than those provided by the GPS time series. The weighted mean (WM) of the differences, respectively of 0.7 mm/ yr (reference model *ICE-6G_C-VM5a*) and 0.9 mm/yr (reference model W12A_v1), highlights the fact that the predicted uplift rates at GPS sites are overestimated.

The discrepancies between predicted and detected uplifts are likely related to the tectonic features of the region, which are also of interest to this work. In particular, the highest and lowest observed values are not confirmed by the models (Fig. 5).

Fig. 5 Comparison between vertical rates as estimated by GPS observations on VLNDEF sites (blue diamonds) and GIA models: ICE 6G C VM5a (red triangles); W12A (yellow circles). Error bars are $\pm\sigma$.

Both the GPS-derived movements and those predicted by GIA models show positive vertical rates westward. Northward, GPS-derived uplift rates and values predicted by the above mentioned GIA models are not in agreement, even though the very small absolute values do not facilitate such validation. Again, this disagreement could be due to the relative motion among the few sites experiencing tectonic activity in the VL region (Fig. 6).

Fig. 6 - The uplift movements of VLNDEF sites in the NVL area predicted from the models and observed by GPS. ICE 6G C-VM5a (red triangles); W12A_v1 (yellow circles); GPS observations (blue diamonds). Error bars are $\pm\sigma$.

Table 4 - Predicted rates (v_u) and differences (Δv_u) between the estimated and observed values at each VLNDEF station. The weighted mean (WM) and the weight root mean square (WRMS) of the residuals show the degree of agreement between the solutions.

5 - Discussion

Looking at the figure of the absolute velocities (Fig. 2), it is possible to observe that the GNSS stations of the VLNDEF network are iso-oriented in a direction towards SE and have comparable modules. The horizontal residual rates, calculated after the Euler pole estimates (59.536°S, 52.417°E, 0.220°/Myr), are obtained by subtracting the rigid movement of the Antarctic plate from the absolute velocity of the stations (Fig. 3). The mean residual velocities of the VLNDEF sites are generally small with respect to the absolute velocities.

To identify GNSS sites with significant movements, the residual velocities were analyzed with respect to the corresponding errors. Considering the rates with lower values than the sigma, not significative for the geodynamic interpretation, 19 points show meaningful movements: along the horizontal (VL02, VL03, VL10, VL14, VL23, VL32. VLHG), along the vertical (VL04, VL05, VL07, VL18), and in 3D components (VL06, VL08, VL12, VL19, VL21, VL22, VL29, VL30).

Residual velocities reported from the above mentioned sites could provide information about the presence of local or regional deformation phenomena, not accounted for in the rigid plate movement mechanism.

The average rate of observed uplift in VL is negligible (0.5±0.97 mm/yr) but few sites show significant movements. From the spatial point of view, a general increase in the uplift rates was found westward, toward the areas with maximum ice-

load. These vertical movements show the same trend as the GIA models but with lower values. Northward (Fig. 6) the observed up rate is influenced by the few sites which register neotectonic displacements.

The high quality of the GPS up components permits in inference of information concerning tectonic-related vertical movements.

Both the absolute values and the residuals from their comparison with the GIA models show a relative vertical displacement between the north and east sectors and the southern one. The first block is characterized by a relative uplifting with respect to the southern one, considering the post-glacial rebound effect from the GIA models. An exception, VL06, shows a relative uplift with respect to the surrounding stations (e.g. TNB1, VL10, VL08 and VL07). This tectonic activity can be easily ascribed to the active Mt. Melbourne Volcano, on top of which the station is located. The boundary between the two zones is located at the exactly latitude where Tucker Fault's SE termination meets the central Leap Year Fault, Evans Nevè and the central Aviator Fault (Fig. 7).

Fig. 7 - Active tectonic uplifting in Victoria Land. Vertical rates computed by subtracting ICE up rates from GPS observed values. Pink area denotes the relatively uplifting sector. The light blue one corresponds to the relatively downlifting sector. Vertical movements are framed in the neotectonic model from Dubbini et al. (2010) which showed extensional/transtensional regimes along segments of the Cape Adare, Tucker, Leap Year, and Aviator faults, here highlighted in yellow segments. Extensional reactivation of transversal normal faults is inferred and indicated with dashed yellow lines.

Along this corridor, Dubbini et al., (2010), using the residual horizontal components of the GPS in the period 1999-2006, proposed active extension (transtension) along the Tucker and Leap Year Faults a horizontal displacement velocities between 2 and 5 mm/yr. Results from the up component presented in this paper confirm the presence of active extensional faulting along the SE segment of the Tucker Fault and the central segment of the Leap Year Fault.

A vertical displacement is also active along the fault connecting Tucker to the Tasman Fracture Zone II. A vertical displacement, with SW down-throw, can be also be inferred, in the central Aviator Fault where horizontal displacements are not present (Fig. 7). The central sector of the Lanterman Fault, near VL12, shows a vertical offset with NE down-throw. Along the boundary between the uplifting and downlifting sectors, transverse normal faults are active and

accompanies the down-throw of the southern sector (Fig.7). The high-up component present in VL23 may relate to the activity of the Cape Adare Fault along its SE part.

The new up component analysis allows a complete definition of the tectonic frame of Victoria Land. This includes the relative up displacement of the Victory Block, with respect to the Rennick Block as well as that of the northern Victory Block with respect to the Admiralty Block, which in turn is uplifting with respect to the southern Victory Block (Fig. 7). The Lanterman Block (VL21), characterized by strong horizontal displacements, is downlifting with respect to the northern sector of the Victory Block. The vertical uplifting computed from VL06 confirms the activity of the Mt. Melbourne Volcano. It is worth noting that a similar behavior can be observed on the absolute up displacements, without applying GIA models. Actually, these corrections reduce the vertical velocities among blocks of about 1 mm/yr. This new GPS dataset further strengthens the presence of active tectonics in the region and its role in the relative (small) movements among the rigid crustal blocks that form the VL region. The inland SE continuation of the Tasman Fracture Zone corresponds to the uplifting sector of VL. The present-day activity of this fracture zone, as proven by intense seismicity, may continue in the northern sector of VL and be responsible for the observed tectonic uplifting. As reported in the introduction, large earthquakes may have contributed to the observed geodetic vertical velocities, thus reducing/enhancing the role played by Victoria Land faults, even if no clear evidence is present in our dataset.

6 - Conclusion

The VLNDEF network, periodically active since 1999, is able to detect reliable vertical rates at the stations and to separate the local from the regional horizontal displacements, as a function of the computed Euler pole. The periodical solutions which are characterized by improved accuracy are confirmed by the length of the time series and detected, applying different processing strategies (Capra et al., 2007; Dubbini et al., 2010; Negusini et al. 2005, Zanutta et al. 2008).

Differences in vertical rates highlighted the presence of transtension across the Tucker and Leap Year faults, resulting from the relative uplift of the N-NE sector of the VL. This may easily relate to the SE propagation of the activity along the Tasman Fracture Zone.

The differences in tectonic-related horizontal velocities between our results and those previously proposed by Dubbini et al. (2010) may relate to the Euler pole re-computations that included the VLNDEF stations. The horizontal velocity

differences may also reflect changes in the plate motions of large earthquakes over the last couple decades, although the software used tends to eliminate the steps in the series corresponding to the these events.

Even though the displacements from GPS observation represent a fundamental verification of outcomes from GIA models, the direct comparison between GPS-derived displacements and outcomes from GIA modelling is not an easy task. Certainly, load variations, the choice of upper-mantle viscosity and thickness of the lithosphere, may improve, thanks to the availability of dense geodetic measurements derived from the VLNDEF project. However, some signals are still left unconsidered by authors and deserve further efforts to quantify of their magnitude and potential bias: both of these were introduced in the comparison between the results provided by GIA models and GPS-derived displacements, in the vertical as well as horizontal components. In particular, some signals have been introduced in the present paper and recent scientific literature. The effects of elastic deformations and recent changes in polar motion need careful evaluation along with an even more detailed reconstruction of melt-rates occurring over the last two decades. The northern VL is not within the areas most involved in ice-melting processes but possibly signals in the far field might also affect the displacements from GPS data processing. A few tenths of mm/yr were predicted by available models of the investigated areas. A better estimation of these signal values represents a stringent need for future work.

Acknowledgements

Part of this work was supported by the Italian National Program for Antarctic Research (PNRA, Programma Nazionale di Ricerche in Antartide). Many researchers contributed to the field activities. We thank W. Richard Peltier and Pippa Whitehouse for providing their models. We acknowledge contribution from the International GNSS Service, POLENET, UNAVCO. We are grateful to reviewer Matt King for extensive insight and suggestions on the submitted manuscript. Also we thank to an anonymous reviewer who helped to improve the paper and to the Editor Irina Artemieva for her assistance. Figures 1, 2, 3, 4, 7 were produced with the Generic Mapping Tool software (Wessel & Smith 1991).

References

Altamimi, Z., Collilieux, X., Métivier, L., 2011. ITRF2008: An improved solution of the international terrestrial reference frame. J. Geodesy, 85(8), 457–473, doi: 10.1007/s00190-011-0444-4.

Altamimi, Z., Metivier, L., Collilieux, X., 2012. ITRF2008 plate motion model, J. Geophys. Res., 117, doi:10.1029/2011JB008930.

Amalvict, M., Willis, P., Wöppelmann, G., Ivins, E. R., Bouin, M.-N., Testut, L., Hinderer, J., 2009. Isostatic stability of the East Antarctic station Dumont d'Urville from long-term geodetic observations and geophysical models. Polar Res., 28(2), 193–202, doi:10.1111/j.1751-8369.2008.00091.x.

Argus, D. F., 2012. Uncertainty in the velocity between the mass center and surface of Earth, J. Geophys. Res., 117(B10), 1–15. doi:10.1029/2012JB009196.

Argus, D.F., Peltier, W.R., Drummond, R., Moore, A.W., 2014. The Antarctica component of postglacial rebound model ICE-6G_C (VM5a) based upon GPS positioning, exposure age dating of ice thicknesses, and relative sea level histories. Geophys. J. Int., 198(1), 537-563, doi:10.1093/gji/ggu140.

Bevis, M., Kendrick, E., Smalley, R. Jr., Dalziel, I., Caccamise, D., Sasgen, I., Helsen M., Taylor F. W., Zhou H., Brown A., Raleigh, D., Willis, M., Wilson, T., Konfal, S., 2009. Geodetic measurements of vertical crustal velocity in West Antarctica and the implications for ice mass balance. Geochem. Geophys. Geosyst., 10, Q10005, doi:10.1029/2009GC002642.

Boehm, J., Werl, B., Schuh, H., 2006. Troposphere mapping functions for GPS and very long baseline interferometry from European Centre for medium-range weather forecasts operational analysis data. J. Geophys.Res., Solid Earth, 111(B2), Art. ID B02406, doi: 10.1029/2005JB003629.

Bouin, M. N., Vigny, C., 2000. New constraints on Antarctic plate motion and deformation from GPS data. J. Geophys. Res., 105(B12), 28,279–28,293, doi:10.1029/2000JB900285.

Burton-Johnson, A., Black, M., Fretwell, P. T., Kaluza-Gilbert, J., 2016. An automated methodology for differentiating rock from snow, clouds and sea in Antarctica from Landsat 8 imagery: a new rock outcrop map and area estimation for the entire Antarctic continent. The Cryosphere, 10, 1665–1677. doi:10.5194/tc-10-1665-2016.

Capra, A., Gandolfi, S., Mancini, F., Sarti, P., Vittuari, L., 2001. VLNDEFproject: geodetic contribution to geodynamics study of Victoria Land, Antarctica. IAG Symp., GGG2000 Gravity, Geoid and Geodynamics 2000, ed. M. G. Sideris, Springer, 123, 379-385, ISBN 3-540-42469-5.

Capra, A., Mancini, F., Negusini, M., 2007. GPS as a geodetic tool for geodynamic in Northern Victoria Land, Antarctica. Antarct. Sci., 19(1), 107-114, doi: 10.1017/s0954102007000156.

Capra, A., Dubbini, M., Galeandro, A., Gusella, L., Zanutta, A., Casula, G., Negusini, M., Vittuari, L., Sarti, P., Mancini, F., Gandolfi, S., Montaguti, S., Bitelli, G., 2008. VLNDEF Project for Geodetic Infrastructure Definition of Northern Victoria Land, Antarctica. In Geodetic and Geophysical Observations in Antarctica, edited by A. Capra and R. Dietrich. Springer-Verlag Berlin Heidelberg, doi: 10.1007/978-3-540-74882-3_3.

Dach, R., Lutz, S., Walser, P., Fridez P., 2015. Bernese GNSS Software Version 5.2. User manual, Astronomical Institute, University of Bern, Bern Open Publishing, doi: 10.7892/boris.72297; ISBN: 978-3-906813-05-9.

Delle Donne, D., Harris, A. J. L., Ripepe, M., Wright, R. 2010. Earthquake-induced thermal anomalies at active volcanoes. Geology, 38(9):771–774. doi: 10.1130/G30984.1.

Dietrich, R., Rülke, A., Scheinert, M., 2005. Present-day vertical crustal deformations in West Greenland from repeated GPS observations. Geophys. J. Int.163, 865–874, doi: 10.1111/j.1365-246X.2005.02766.x.

Dong, P., Fang, P., Bock, Y., Cheng, M. K., Miyazaki, S., 2002. Anatomy of apparent seasonal variations from GPS-derived site position time series. Journal of Geophysical Research, 107(B4). doi: 10.1029/2001JB000573.

Dubbini, M., Cianfarra, P., Casula, G., Capra, A., Salvini, F., 2010. Active tectonics in northern Victoria Land (Antarctica) inferred from the integration of GPS data and geologic setting. J. Geophys. Res., Solid Earth, 115(B12), doi: 10.1029/2009JB007123.

Egbert, G.D., Erofeeva, S.Y., 2002. Efficient Inverse Modeling of Barotropic Ocean Tides. J. Atmos. Oceanic Technol. 19, 183204. doi: http://dx.doi.org/10.1175/1520-0426(2002)019<0183:EIMOBO>2.0.CO;2

King, M.A., Altamimi, Z., Boehm, J., Bos, M., Dach, R., Elosegui, P., Fund, F., Hernández-Pajares, M., Lavallée, D., Mendes Cerveira, P.J., Penna, N., Riva, R.E.M., Steigenberger, P., Van Dam T., Vittuari, L., Williams, S., Willis, P., 2010. Improved Constraints to Models of Glacial Isostatic Adjustment: A Review of the Contribution of Ground-based Geodetic Observations. Surv. Geophys., 31(5), 465-507, doi: 10.1007/s10712-010-9100-4.

King, M.A., Watson, C.S., 2014. Geodetic vertical velocities affected by recent rapid changes in polar motion. Geophys. J. Int., 199(2), 1161–1165, doi: 10.1093/gji/ggu325.

King, M.A., Santamarìa-Gòmez, A., 2016. Ongoing deformation of Antarctica following the Great Earthquakes. Geophys. Res. Lett., 43, 1918–1927, doi: 10.1002/2016GL067773.

King, M.A, Whitehouse, P.L., Van der Wal., W., 2016. Incomplete separability of Antarctic plate rotation from glacial isostatic adjustment deformation within geodetic observations. Geophys J Int. 2016;204, 324–30. doi:10.1093/gji/ggv461.

Klemann, V. & Martinec, Z., 2011. Contribution of glacial-isostatic adjustment to the geocenter motion, Tectonophysics, 511, 99–108. doi:10.1016/j.tecto.2009.08.031

Lagler, K., Schindelegger, M., Böhm, J., Krásná, H., Nilsson, T., 2013. GPT2: Empirical slant delay model for radio space geodetic techniques. Geophys. Res. Lett., 40(6), 1069–1073, doi: 10.1002/grl.50288.

Letellier, T., 2004. Etude des ondes de marée sur les plateaux continentaux. Ph.D. thesis, Université III Paul Sabatier.

Mancini, F., 2001. Geodetic activities: a new GPS network for crustal deformation control in northern Victoria Land. Terra Antartica Reports 5, 23–28, ISBN 88-900221-6-7.

Márquez-Azúa, B., Cabral-Cano, E., Correa-Mora, F., DeMets, C., 2004. A model for Mexican neotectonics based on nationwide GPS measurements, 1993–2001. Geofis. Int. 43(3), 319–330.

Martín-Español, A., Zammit-Mangion, A., Clarke, P.J., Flament, T., Helm, V., King, M.A., Luthcke, S.B., Petrie, E., Rémy, F., Schön, N., Wouters, B., Bamber, J.L., 2016. Spatial and temporal Antarctic Ice Sheet mass trends, glacio-isostatic adjustment, and surface processes from a joint inversion of satellite altimeter, gravity, and GPS data, J. Geophys. Res. Earth Surf., 121, 182–200. doi:10.1002/2015JF003550.

Mao, A., Harrison, C.G.A., Dixon, T.H., 1999. Noise in GPS coordinate time series. J. Geophys. Res., 104(B2), 2797–2816, doi:10.1029/1998JB900033.

Mitrovica, J.X., Vermeersen, B.L.A., 2002. Glacial Isostatic Adjustment and the Earth System, in Ice Sheets Sea Level and the Dynamic Earth. AGU Geodyn. Res. Ser., 29.

Mitrovica, J.X., Milne, G.A., 2003. On post-glacial sea level: I. General theory. Geophys. J. Int. 154(2), 253-267, doi: 10.1046/j.1365-246X.2003.01942.x.

Mitrovica, J.X., Wahr, J., Matsuyama, I., Paulson, A., 2005. The rotational stability of an ice-age earth. Geophys. J. Int. 161(2), 491-506, doi: 10.1111/j.1365-246X.2005.02609.x.

Negusini, M., Mancini, F., Gandolfi, S., Capra, A., 2005. Terra Nova Bay GPS permanent station (Antarctica): data quality and first attempt in the evaluation of regional displacement. Journal of Geodynamics, 39, 81–90, doi: 10.1016/j.jog.2004.10.002.

Negusini, M., Petkov, B. H., Sarti, P., Tomasi, C., 2016. Ground-Based Water Vapor Retrieval in Antarctica: An Assessment. IEEE T. Geosci. Remote, 54 (5), doi: 10.1109/TGRS.2015.2509059.

Nettles, M., Wallace, T. C., Beck, S. L., 1999. The March 25, 1998 antarctic plate earthquake. Geophys. Res. Lett., 26(14), 2097–2100, doi:10.1029/1999GL900387.

Nield, G.A., Barletta, V.R., Bordoni, A., King, M.A., Whitehouse, P.L., Clarke, P.J., Domack, E., Scambos, T.A., Berthier, E., 2014. Rapid bedrock uplift in the Antarctic Peninsula explained by viscoelastic response to recent ice unloading. Earth Planet. Sci. Lett. 397, 32e41. http://dx.doi.org/10.1016/j.epsl.2014.04.019.

Ostini, L., Dach, R., Meindl, M., Schaer, S., Hugentobler, U., 2008. FODITS: A new tool of the Bernese GPS Software. In Torres, J. A. and H. Hornik, editors, Subcommission for the European Reference Frame (EUREF).

Ostini, L., Dach, R., Schaer, S., Hugentobler, U., Meindl, M., Beutler, G., 2010. Time series analysis using FODITS. In COST ES0701 WG 1-3 meeting, Nottingham, UK, Mar. 2010. URL U:\Groups\gps\PosterNottiingham2010\PosterNottingham2010Ati.

Ostini, L., 2012. Analysis and Quality Assessment of GNSS–Derived Paramter Time Series. PhD thesis, Astronomical Institute, University of Bern, Bern, Switzerland.

Peltier, W.R., 2004. Global glacial isostasy and the surface of the ice-age Earth: the ICE-5G (VM2) Model and GRACE, Annu. Rev. Earth planet. Sci., 32, 111–149, doi: 10.1146/annurev.earth.32.082503.144359.

Peltier, W.R., Argus, D.F., Drummond, R., 2015. Space geodesy constrains ice-age terminal deglaciation: The global ICE-6G_C (VM5a) model. J. Geophys. Res. Solid Earth, 120, 450-487, doi:10.1002/2014JB011176.

Purcell, A., Tregoning, P., Dehecq, A. 2016. An assessment of the ICE6G_C(VM5a) glacial isostatic adjustment model. Journal of Geophysical Research: Solid Earth, 121 (5), pp. 3939-3950. DOI: 10.1002/2015JB012742

Reading, A. M., 2007. The seismicity of the Antarctic plate. Geol. Soc. Am. Spec. Pap., 425, 285–298, doi:10.1130/2007.2425(18).

Rietbroek, R., Brunnabend, S.-E., Kusche, J.&Schr¨oter, J., 2012. Resolving sea level contributions by identifying fingerprints in time-variable gravity and altimetry, J. Geodyn., 59-60, pp. 72-8, doi:10.1016/j.jog.2011.06.007.

Riva R.E.M, Frederikse, T., King, M.A., Marzeion, B., van den Broeke, M., 2016. Brief Communication: The global signature of post-1900 land ice wastage on vertical land motion. The Cryosphere Discuss., doi:10.5194/tc-2016-274.

Rothacher M., Angermann, D., Artz, T., Bosch, W., Drewes, H., Gerstl, M., Kelm, R., König, D., König, R., Meisel, B., Müller, H., Nothnagel, A., Panafidina, N., Richter, B., Rudenko, S., Schwegmann, W., Seitz, M., Steigenberger, P., Tesmer, S., Tesmer, V., Thaller, D., 2011. GGOS-D: Homogeneous reprocessing and rigorous combination of space geodetic observations. J. Geodesy, 85, 10, 679–705, doi: 10.1007/s00190-011-0475-x.

Saleh, M., Becker, M., 2015. New constraints on the Nubia–Sinai–Dead Sea fault crustal motion. Tectonophysics, 651–652, 79–98, doi: 10.1016/j.tecto.2015.03.015.

Salvini, F., Storti F., 1999. Cenozoic tectonic lineaments of the Terra Nova Bay region, Ross Embayment, Antarctica. Global Planet. Change, 23, 129–144. DOI: 10.1016/S0921-8181(99)00054-5.

Salvini, F., Brancolini, G., Busetti, M., Storti, F., Mazzarini, F., Coren, F., 1997. Cenozoic geodynamics of the Ross Sea region, Antarctica: crustal extension, intraplate strike-slip faulting, and tectonic inheritance. J. Geophys. Res., 102(24), 669–696.

Simon, K. M., James, T. S., Ivins, E. R., 2010. Ocean loading effects on the prediction of Antarctic glacial isostatic uplift and gravity rates. J. Geod., 84(5), 305–317, doi:10.1007/s00190-010-0368-4.

Steffen, H., Wu, P. 2014. The sensitivity of GNSS measurements in Fennoscandia to distinct three-dimensional upper-mantle structures. Solid Earth, 5, 557–567, doi:10.5194/se-5-557-2014.

Steigenberger, P, Rothacher, M, Dietrich, R, Fritsche, M, Rülke, A, Vey, S., 2006. Reprocessing of a global GPS network. J Geophys Res 111(B5), B05402, doi: 10.1029/2005JB003747.

Steigenberger, P., Rothacher, M., Fritsche, M., Ruelke, A., Dietrich, R., 2009. Quality of reprocessed GPS satellite orbits. J. Geodesy, 83(3-4), 241–248, doi: 10.1007/s00190-008-0228-7.

Tesmer, V., Steigenberger P., Rothacher, M., Boehm, J., Meisel, B., 2009. Annual deformation signals from homogeneously reprocessed VLBI and GPS height time series. J. Geodesy, 83(10), 973–988, doi: 10.1007/s00190-009-0316-3.

Thomas, I.D., King, M.A., Bentley, M.J., Whitehouse, P.L., Penna, N.T., Williams, S.D.P., Riva, R.E.M., Lavallee D.A., Clarke P. J., King E., Hindmarsh R. C. A., Koivula, H., 2011. Widespread low rates of Antarctic glacial isostatic adjustment revealed by GPS observations. Geophys. Res. Lett., 38(22), L22302, doi: 10.1029/2011GL049277.

Torsvik, T.H., Müller, R.D., Van Der Voo, R., Steinberger, B., Gaina, C., 2008. Global plate motion frames: Toward a unified model. Rev. Geophys., 46(3), doi:10.1029/2007RG000227.

Watson, C, Burgette, R, Tregoning, P, White, N, Hunter, J, Coleman, R, Handsworth, R, Brolsma, H., 2010. Twentieth century constraints on sea level change and earthquake deformation at Macquarie Island. Geophys. J. Int., 182(2), 781–796, doi:10.1111/j.1365-246X.2010.04640.x.

Wessel, P. Smith, W.H.F., 1991. Free software helps map and display data. EOS, Trans. Am. Geophys. Un., 72(41), 441–446, doi: 10.1029/90EO003319.

Whitehouse, P.L., Bentley, M.J., Le Brocq, A.M., 2012a. A deglacial model for Antarctica: geological constraints and glaciological modelling as a basis for a new model of Antarctic glacial isostatic adjustment. Quat. Sci. Rev., 32, 1–24, doi: 10.1016/j.quascirev.2011.11.016.

Whitehouse, P.L., Bentley, M.J., Milne, G.A., King, M.A., Thomas, I.D., 2012b. A new glacial isostatic adjustment model for Antarctica: calibrated and tested using observations of relative sea-level change and present-day uplift rates. Geophys. J. Int., 190, 1464-1482, doi:10.1111/j.1365-246X.2012.05557.x.

Williams, S.D.P., 2003. The effect of coloured noise on the uncertainties of rates estimated from geodetic time series. J. Geodesy, 76, 483–494, doi: 10.1007/s00190–002–0283–4.

Williams, S.D.P., Bock, Y., Fang, P., Jamason, P., Nikolaidis, R.M., Prawirodirdjo, L., Miller, M., Johnson, D.J., 2004. Error analysis of continuous GPS position time series. J. Geophys. Res., 109, B03412, doi:10.1029/2003JB002741.

Zanutta A., Vittuari L., Gandolfi S., 2008. Geodetic GPS-based analysis of recent crustal motions in Victoria Land (Antarctica). Global Planet. Change, 62/1-2, 115-131, doi: 10.1016/j.gloplacha.2008.01.001, 0921-8181.

Zhang, J., Bock,Y., Johnson, H., Fang, P.,Williams, S., Genrich, J., Wdowinski, S., Behr, J., 1997. Southern California permanent GPS geodetic array: error analysis of daily position estimates and site velocities. J. Geophys. Res., 102(B8), 18 035–18 055, doi: 10.1029/97JB01380.

.

List of figures

Fig.1. GNSS Antarctic stations (IGS, POLENET) used in this paper. The VLNDEF network is represented in the upper - right inset.

Fig. 2. Victoria Land absolute velocities.

Fig. 3. Victoria Land horizontal relative velocities with respect to VLNDEF plate model. The very small displacement vectors indicate the general agreement of the VLNDEF model with the Antarctic plate movement, except for some points of the northern part, which confirm the influence of displacements due to tectonic patterns across the region.

Fig. 4. Predictions by postglacial rebound models across the NVL and GPS observed uplift rates. a) ICE-6G_C-VM5a (Argus et al., 2014); b) W12A_v1 (Whitehouse et al., 2012a,b). The circles indicate the difference ranges between the predicted and the observed vertical rates.

Fig. 5 Comparison between vertical rates as estimated by GPS observations on VLNDEF sites (blue diamonds) and GIA models: ICE 6G C VM5a (red triangles); W12A (yellow circles). Error bars are $\pm\sigma$.

Fig. 6 - The uplift movements of VLNDEF sites in the NVL area predicted from the models and observed by GPS. ICE 6G C-VM5a (red triangles); W12A_v1 (yellow circles); GPS observations (blue diamonds). Error bars are $\pm\sigma$.

Fig. 7 - Active tectonic uplifting in Victoria Land. Vertical rates computed by subtracting ICE up rates from GPS observed values. Pink area denotes the relatively uplifting sector. The light blue one corresponds to the relatively downlifting sector. Vertical movements are framed in the neotectonic model from Dubbini et al. (2010) which showed extensional/transtensional regimes along segments of the Cape Adare, Tucker, Leap Year, and Aviator faults, here highlighted in yellow segments. Extensional reactivation of transversal normal faults is inferred and indicated with dashed yellow lines.

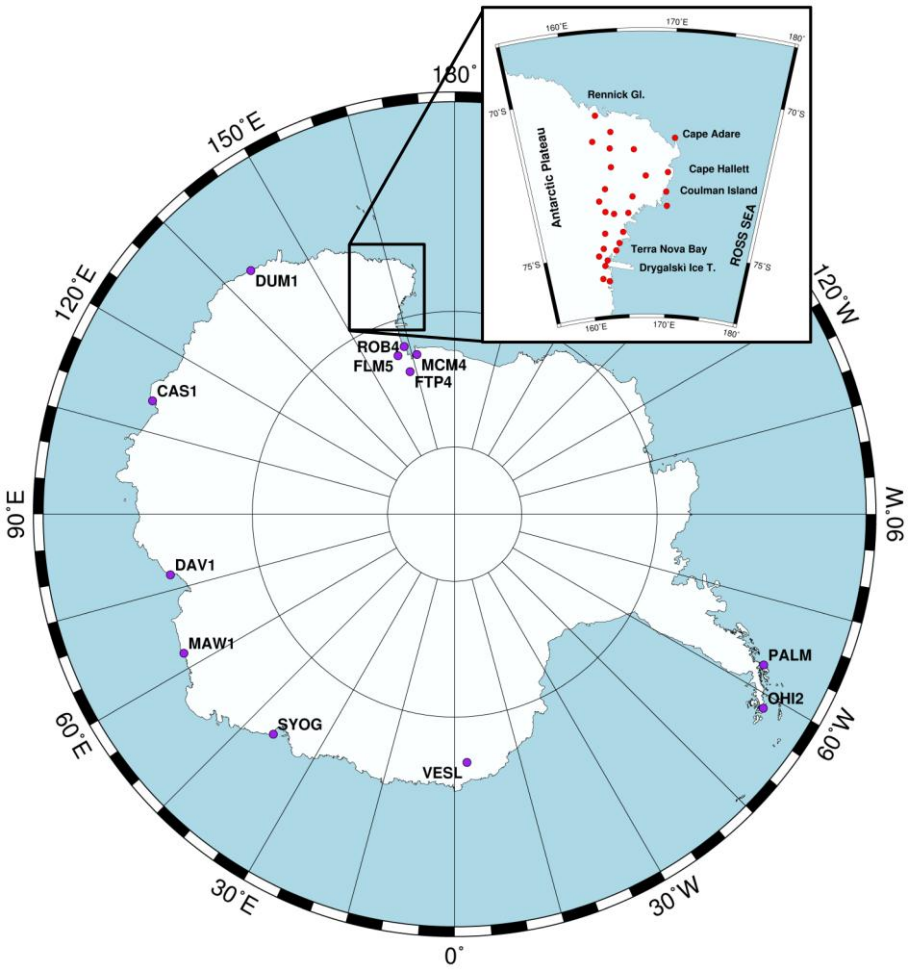

Fig. 1

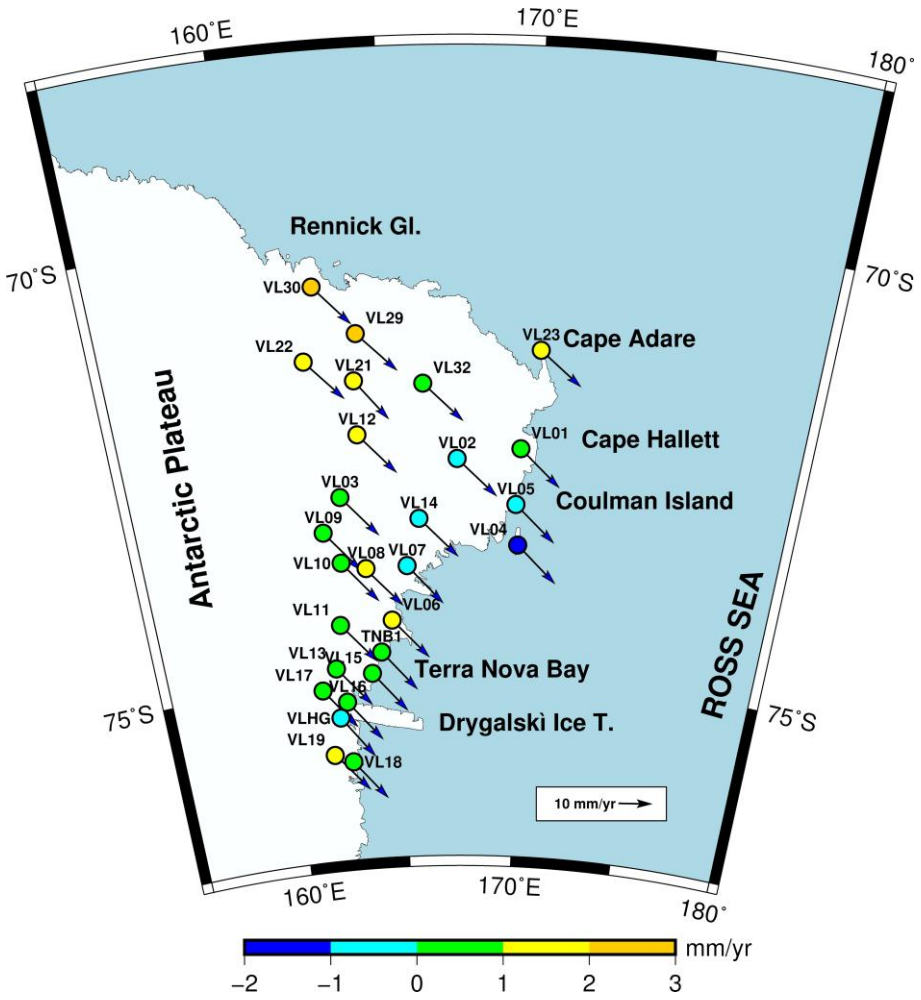

Fig. 2

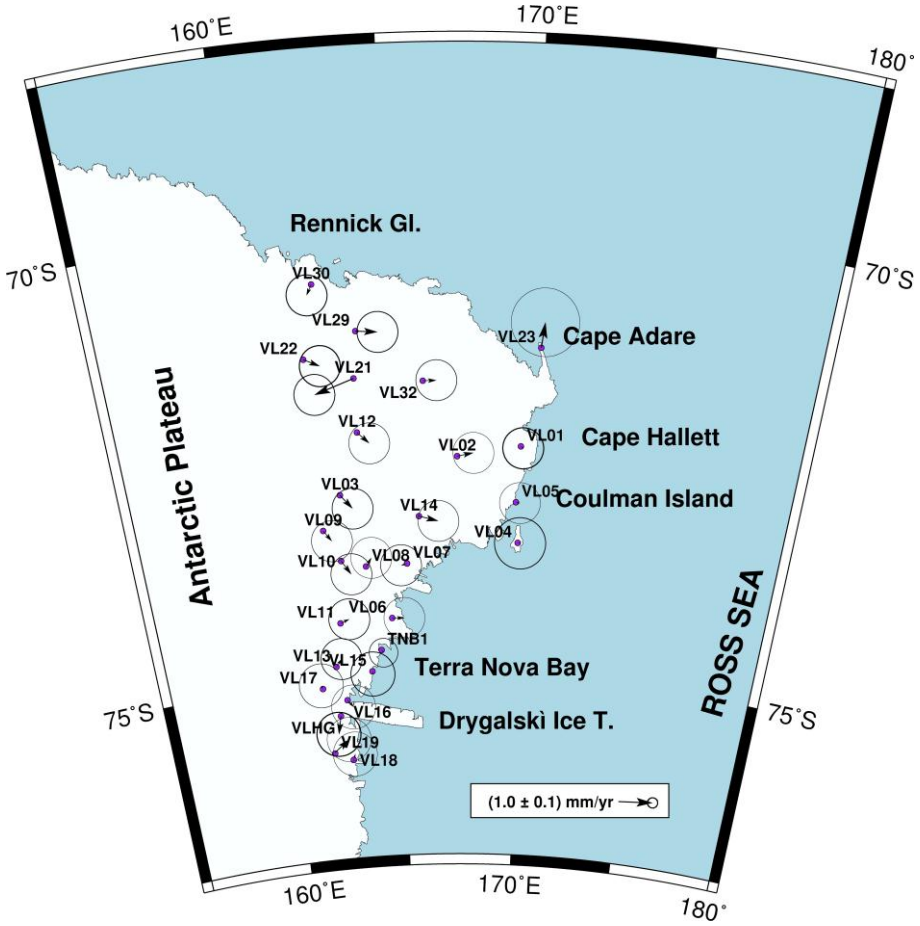

Fig.3

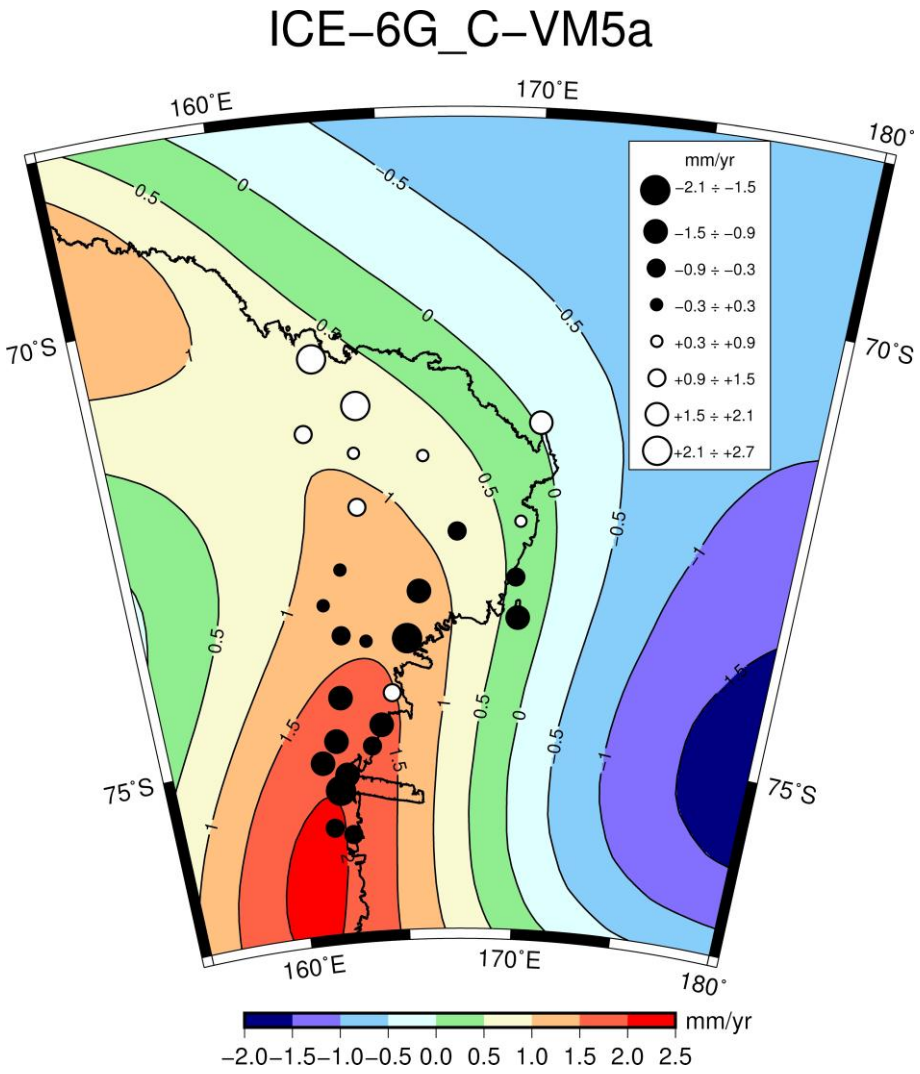

Fig. 4a

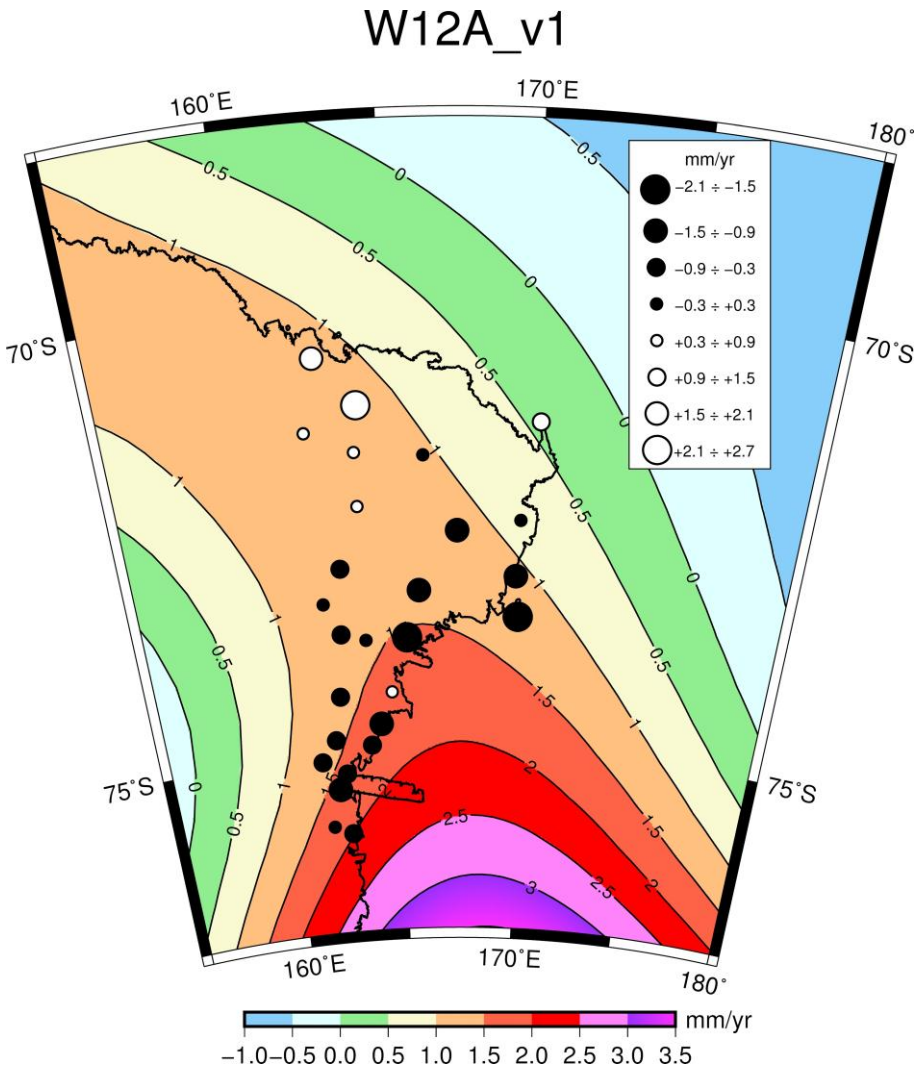

FIG. 4b

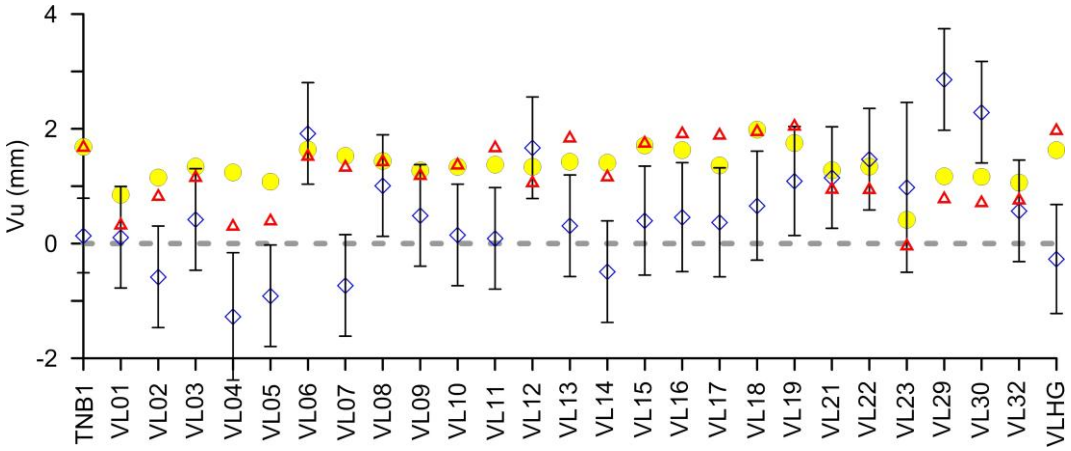

Fig. 5

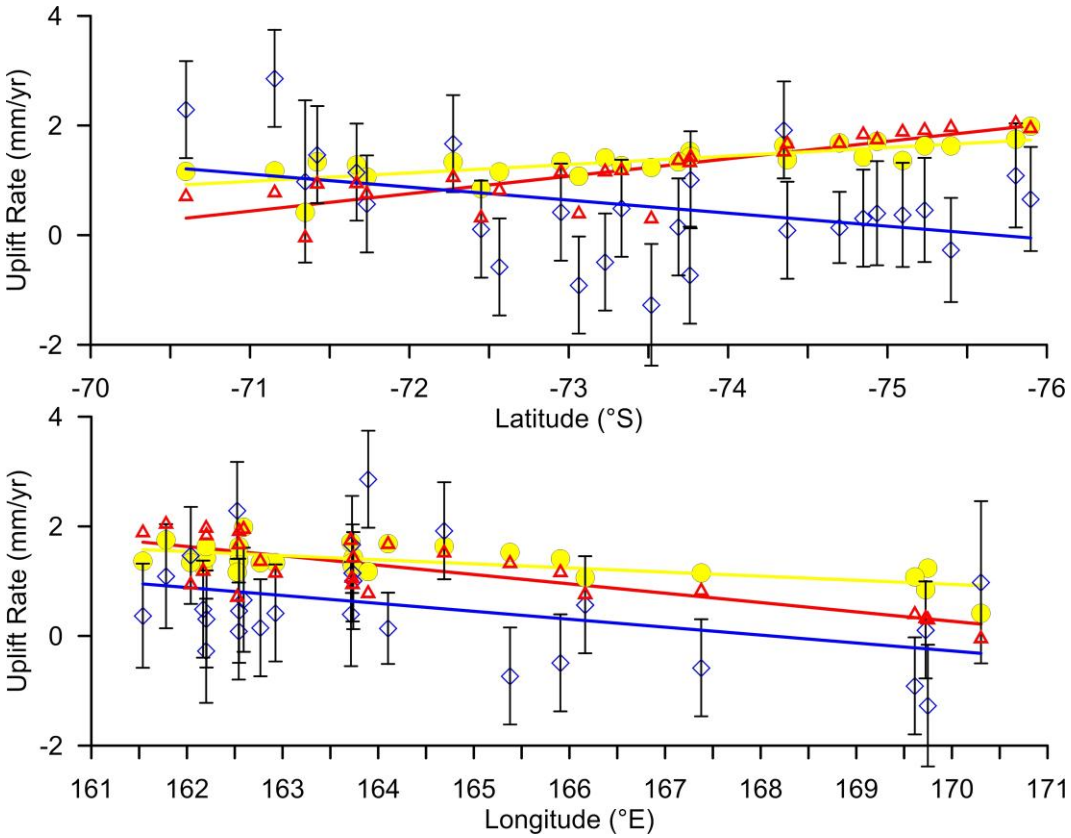

Fig. 6

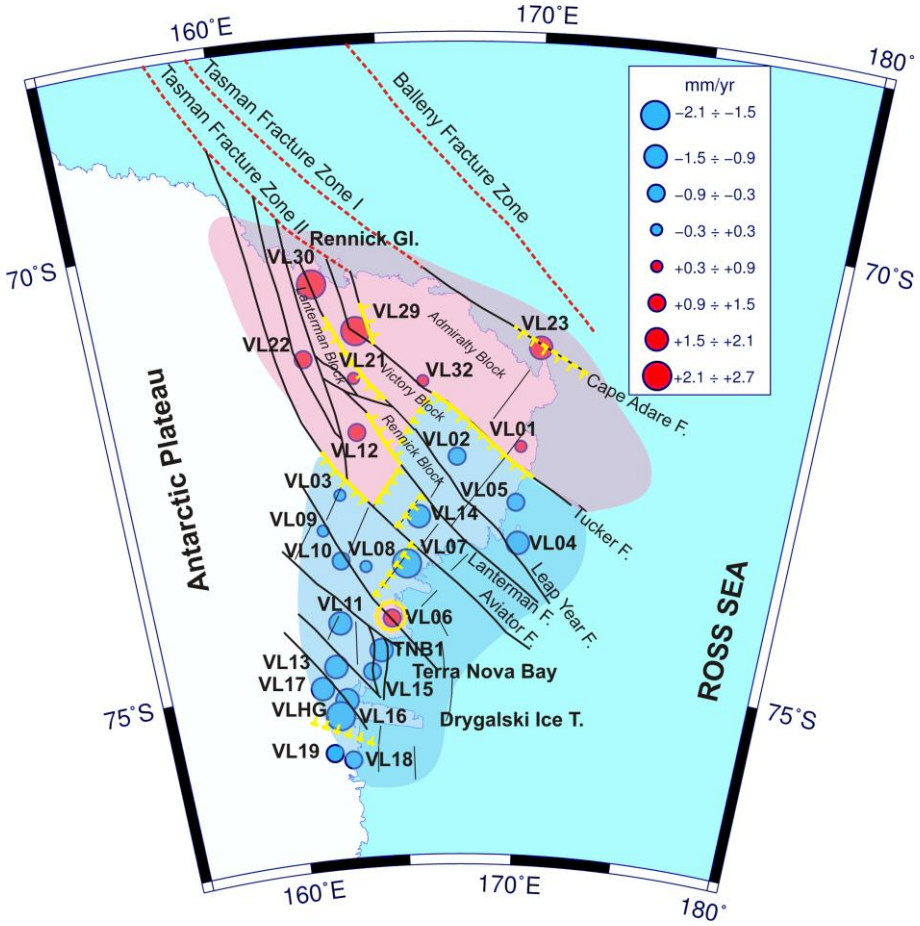

Fig. 7

List of tables

Table 1 - GNSS sites in the VL region. For each year the number of daily observations is given. The last two columns indicate the accumulated total amount of daily observations (Tot) and the number of repetitions (Rep).

ID	99	00	02	03	04	05	06	07	08	09	10	11	12	13	14	15	Tot.	Rep
VL01	1	-	18	88	63	3	9	-	35	98	102	47	106	136	109	40	855	14
VL02	6	2	1	20	-	4	9	-	-	-	-	-	14	-	16	-	72	8
VL03	6	2	-	16	-	3	19	-	10	-	-	-	12	-	33	-	101	8
VL04	-	-	3	17	-	3	2	-	-	-	16	-	-	-	17	-	58	6
VL05	3	-	21	43	33	26	37	-	48	100	86	117	91	67	118	25	815	14
VL06	-	1	-	15	36	-	17	-	-	-	-	-	21	5	21	25	141	8
VL07	4	5	6	15	-	7	10	-	7	-	15	-	15	-	33	-	117	10
VL08	-	6	-	9	-	-	13	-	9	-	-	-	6	-	4	23	70	7
VL09	6	2	-	19	-	-	13	-	5	-	-	-	9	-	13	-	67	7
VL10	4	4	-	25	34	11	33	-	4	-	-	-	-	-	13	-	128	8
VL11	-	4	-	9	-	-	17	-	-	-	-	4	6	-	13	-	53	6
VL12	6	2	5	52	55	26	36	-	10	-	-	-	7	-	15	40	254	11
VL13	2	7	-	10	-	-	13	-	7	-	7	-	13	-	6	29	94	9
VL14	10	2	-	46	34	26	26	-	5	-	4	-	15	-	10	-	178	10
VL15	-	6	-	19	-	-	7	-	-	2	17	4	14	-	-	26	95	8
VL16	-	8	-	15	11	-	13	-	7	1	5	1	-	-	20	-	81	9
VL17	-	7	-	27	46	-	13	-	-	1	1	5	-	-	7	30	137	9
VL18	-	4	-	11	6	-	13	-	-	1	128	133	53	145	140	40	684	1 0
VL19	-	4	-	9	52	-	11	-	-	1	26	-	-	-	4	8	115	8
VL21	4	1	2	2	-	10	-	-	4	-	3	-	9	-	20	3	58	10
VL22	2	3	5	2	-	5	-	-	-	9	-	-	6	-	21	3	56	9
VL23	-	-	-	40	26	4	2	-	-	-	-	-	13	-	15	-	100	6
VL29	1	3	-	2	-	11	-	-	-	-	-	-	9	-	21	3	53	7
VL30	-	2	3	2	-	5	-	-	-	-	-	-	9	-	11	40	72	7
VL32	2	-	13	2	-	13	9	-	-	-	-	-	16	-	18	-	73	7
VLHG	-	3	-	-	-	22	21	-	-	-	-	-	-	-	-	26	72	4

Table 2 – List of VLNDEF sites with coordinates, absolute and relative velocities along the north and east components (from DOY 349 of 1998 to DOY 040 of 2015) and their estimated uncertainties ($\pm\sigma$).

				Absolute velocities			Relative velocities		Errors		
	Longitude	Latitude	H	v_e	v_n	v_u	v_e	v_n	$\pm\sigma_{ve}$	$\pm\sigma_{vn}$	$\pm\sigma_{vu}$
	(°)	(°)	(m)	(mm/y)	(mm/y)	(mm/y)	(mm/y)	(mm/y)	(mm/y)	(mm/y)	(mm/y)
TNB1	164.10294	-74.69881	72.3	10.1	-11.6	0.1	0.05	-0.08	0.28	0.28	0.65
VL01	169.72507	-72.45014	596.9	11.9	-11.1	0.1	0.07	-0.05	0.40	0.40	0.89
VL02	167.37814	-72.56488	2047.2	11.8	-11.1	-0.6	0.48	0.10	0.40	0.40	0.89
VL03	162.92641	-72.95051	2469.6	10.7	-12.0	0.4	0.34	-0.42	0.40	0.40	0.89
VL04	169.74865	-73.51821	1834.5	11.5	-11.0	-1.3	0.07	-0.01	0.50	0.50	1.11
VL05	169.61219	-73.06307	478.5	11.7	-11.1	-0.9	0.12	-0.02	0.40	0.40	0.89
VL06	164.69065	-74.35000	2671.0	10.6	-11.5	1.9	0.36	-0.01	0.40	0.40	0.89
VL07	165.37930	-73.75990	2039.2	10.4	-11.5	-0.7	-0.18	-0.05	0.40	0.40	0.89
VL08	163.73954	-73.76428	2655.4	10.4	-11.3	1.0	0.18	0.27	0.40	0.40	0.89
VL09	162.16940	-73.33078	2270.5	10.3	-12.0	0.5	0.23	-0.32	0.40	0.40	0.89
VL10	162.76859	-73.68846	2619.4	10.3	-12.0	0.2	0.27	-0.41	0.40	0.40	0.89
VL11	162.54167	-74.37143	2362.3	10.1	-11.5	0.1	0.27	0.10	0.40	0.40	0.89
VL12	163.72700	-72.27444	1933.0	11.1	-11.9	1.7	0.34	-0.34	0.40	0.40	0.89
VL13	162.20497	-74.84780	1460.4	9.7	-11.5	0.3	0.17	0.22	0.40	0.40	0.89
VL14	165.90570	-73.22825	2084.0	11.4	-11.5	-0.5	0.57	-0.15	0.40	0.40	0.89
VL15	163.71567	-74.93426	-28.1	9.9	-11.6	0.4	0.01	-0.08	0.43	0.43	0.95
VL16	162.54549	-75.23256	311.3	9.7	-11.9	0.5	0.16	-0.21	0.43	0.43	0.95
VL17	161.53874	-75.09513	683.5	9.3	-11.6	0.4	-0.04	0.10	0.43	0.43	0.95
VL18	162.59371	-75.89853	58.0	9.4	-11.5	0.7	0.06	0.17	0.43	0.43	0.95
VL19	161.78162	-75.80497	809.8	9.6	-11.4	1.1	0.45	0.35	0.43	0.43	0.95
VL21	163.73294	-71.66866	1899.4	9.7	-12.0	1.2	-1.18	-0.42	0.40	0.40	0.89
VL22	162.04044	-71.42187	274.9	11.2	-11.9	1.5	0.47	-0.23	0.40	0.40	0.89
VL23	170.30467	-71.34582	1119.0	12.3	-10.2	1.0	0.09	0.76	0.67	0.67	1.48
VL29	163.89628	-71.15408	1624.5	11.8	-11.6	2.9	0.65	-0.06	0.40	0.40	0.89
VL30	162.52514	-70.59872	1491.5	10.9	-12.0	2.3	-0.16	-0.31	0.40	0.40	0.89
VL32	166.16457	-71.73310	1784.0	11.8	-11.3	0.6	0.40	0.01	0.40	0.40	0.89
VLHG	162.20172	-75.39797	165.7	9.3	-12.2	-0.3	-0.11	-0.53	0.43	0.43	0.95

Table 3 - Geographic Coordinates and the rotation rate of the Euler pole position projected onto the Southern Hemisphere. ITRF2008 from Altamimi et al. (2012); VLNDEF, this work.

Model	Lat. °N	Lon °E	ω °/Myr
ITRF2008	-58.545±0.29	68.664±0.40	0.209±0.004
VLNDEF	-59.540±0.42	52.370±0.44	0.220±0.002

Table 4 - Predicted rates (v_u) and differences (Δv_u) between the estimated and observed values at each VLNDEF station. The weighted mean (WM) and the weight root mean square (WRMS) of the residuals show the degree of agreement between the solutions.

	ICE-6G v_u (mm/y)	W12 v_u (mm/y)	W12-ob Δv_u (mm/y)	ICE-6G-ob Δv_u (mm/y)
TNB1	1.7	1.7	1.5	1.5
VL01	0.3	0.9	0.7	0.2
VL02	0.8	1.2	1.7	1.4
VL03	1.2	1.3	0.9	0.7
VL04	0.3	1.2	2.5	1.6
VL05	0.4	1.1	2.0	1.3
VL06	1.5	1.6	-0.3	-0.4
VL07	1.3	1.5	2.3	2.1
VL08	1.4	1.4	0.4	0.4
VL09	1.2	1.3	0.8	0.7
VL10	1.4	1.3	1.2	1.2
VL11	1.7	1.4	1.3	1.6
VL12	1.1	1.3	-0.3	-0.6
VL13	1.8	1.4	1.1	1.5
VL14	1.2	1.4	1.9	1.7
VL15	1.7	1.7	1.3	1.3
VL16	1.9	1.6	1.2	1.5
VL17	1.9	1.4	1.0	1.5
VL18	2.0	2.0	1.3	1.3
VL19	2.0	1.8	0.7	1.0
VL21	0.9	1.3	0.1	-0.2
VL22	0.9	1.3	-0.1	-0.5
VL23	0.0	0.4	-0.6	-1.0
VL29	0.8	1.2	-1.7	-2.1
VL30	0.7	1.2	-1.1	-1.6
VL32	0.8	1.1	0.5	0.2
VLHG	2.0	1.6	1.9	2.2
WM			0.9	0.7
WRMS			1.3	1.3